한국해양공학회 2002년도 추계학술대회 논문집 PP.267~272

Estimation of Stress Intensity Factors for 3-Dimensional Surface Defects under Axial Tensile Loads Using the Finite Element Method

BYUNG-YOUNG JEON, Y. V. SATISH KUMAR, AND SUNG-WON KANG
Department of Naval Architecture and Ocean Engineering, Pusan National University, Busan, Korea

KEY WORDS: Stress Intensity Factor, 3-D Surface Defects, Pitting, Corrosion, Finite Element, Cracks

ABSTRACT: *Pitting corrosion is a very common occurrence in marine structures. Therefore, the 3-D finite element analysis is carried out to determine the stress intensity factors at the pit depth and also at the surface of the pit. The pits are modeled as a part of sphere, based on the pit depth and the pit diameter as specified by the Ship Structural Committee. The pit depth and pit diameter are function of the percentage of pitting that the plate is subjected to. A dog-bone shaped specimen is subjected to different intensities of pitting and the stress intensity factors are determined under axial tensile loads.*

1. Introduction

Marine structures are subjected to intense corrosion due to the operating conditions. The corrosion phenomenon is basically divided into two categories i) general corrosion and ii) localized corrosion. The general corrosion is one in which the plate gets corroded uniformly all over whereas in localized corrosion, the corrosion takes place in certain pockets of the plate creating sharp fissures, crevices or cavities. Unlike the general corrosion, the localized corrosion may not be easy to detect since they are camouflaged by the corrosive substance with a deep pit underneath. Therefore, the localized corrosion such as pitting corrosion act as zones of stress concentration and may lead to catastrophic fatigue failure of the structure under the dynamic loads.

Ref.[1-6] have estimated the fatigue life of pitted structures. However, the study is limited to aluminum members and steel members are not considered in the study. Moreover, the pits are of very small size which are typically observed in aircraft structures. In marine structures, the pits are relatively big and the existing formulations for micro pits may not cater to the design needs of the shipbuilding industry. Hoeppner [3] discusses the empirical formulae to estimate the stress intensity factors of pitted steel members. These formulae are based on the assumption that the pit is similar to a surface crack and hence, 3-D effects of the pit geometry are ignored.

In view of this fact, the present paper deals with estimation of stress intensity factors of pitted specimen subjected to different intensities of pitting (from 5% to 20%). The pits manifest as 3-dimensional surface defects on the plate and hence the 3-D finite element method is used to estimate the stress-intensity factors. A dog bone shaped specimen is analysed for various intensities of pitting under axial tensile load. In the present paper, it is assumed that the pit distribution on the specimen is uniform. In uniform distribution, the pits are distributed at regular intervals along the center line of the specimen and all the pits are assumed to be of same size for a given intensity of pitting. The 10 node tetrahedral 3-D finite elements are used to model the specimen. The singular (quarter point node) elements are used in the pits to simulate the crack tip phenomenon in the pit[7].

The stress intensity factors are determined both at the surface of the pit and also at the depth of the pit (from which the cracks are likely to initiate) and the results are compared with those of Newman and Raju [8]. Based on the present investigation, the empirical formulae to estimate the stress intensity factor for 3-dimensional surface defects under axial tensile load are presented as a function of pit depth, pit diameter and specimen thickness.

제1저자 전병영 연락처: 부산시 금정구 장전동 산 30번지 부산대학교 조선해양공학과 051-510-2751 bryanjeon@hotmail.com

2. FE Modeling and Simplified Formula

2.1 Configuration of the Specimen

A dog-bone specimen as shown in Fig. 1 is used in the present analysis. The number of pits on the specimen are based on the intensity of pitting. The intensity of pitting is defined as the percentage of the surface area of the specimen which is subjected to pitting. Three different

intensities of pitting i.e. 5%, 10% and 20% are considered in the present analysis. The size of the pit for any given intensity of pitting is based on the Ship Structural Committee report [9]. The size of the pit i.e. pit depth and pit diameter for different intensities of pitting is shown in Table 1. The pits are modeled as a part of sphere based on the depth and diameter of the pit.

Table 1 Pitting intensity and pit size (㎜)

Pitting Intensity /Pit parameter	5%	10%	20%	30%	40%	50%
Average pit depth	4.55	5.09	5.72	5.52	6.98	7.12
Maximum pit depth	11.39	10.62	11.82	10.13	11.72	11.63
Average pit diameter	14.14	20.75	27.42	32.25	37.73	44.64
Maximum pit diameter	24.72	47.59	49.64	63.66	74.56	73.09

In the present analysis, three different types of specimen each having a different thickness (t=10㎜, 15㎜ and 20㎜) are analysed to investigate the effects of variation in stress intensity factor with respect to thickness.

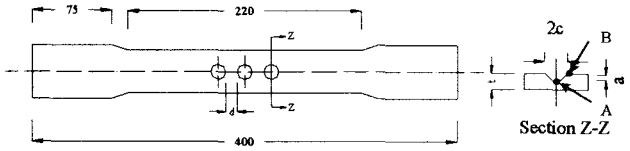

Fig. 1 Configuration of the pitted specimen

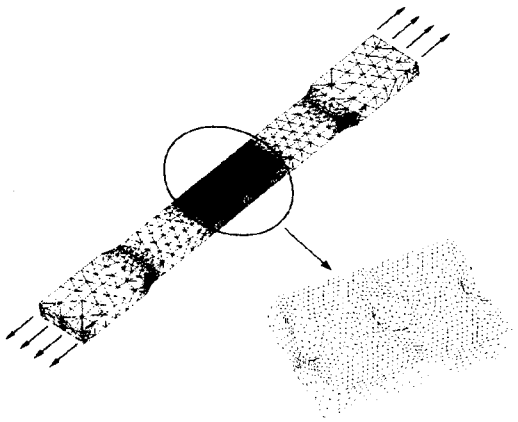

Fig. 2 Finite element model of the pitted specimen

For any given intensity of pitting, all the pits are assumed to be identical having the same depth and diameter. The spacing between the pits is varied from 2mm to 20mm (Fig. 1) to study the effects of multiple pits and pitch of the pits, d.

The 10-node tetrahedral 3-D elements are used for finite element analysis of the specimen. Fig. 2 shows the finite element model used in the analysis. To simulate the condition of infinite stress at the crack tip, the elements along the pit boundary are replaced with singular elements(Fig. 3). The mid-side nodes of these singular elements are shifted to the quarter point, using an interface program, to simulate the crack tip conditions.

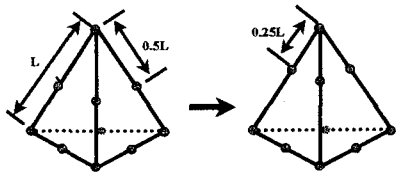

Fig. 3 Tetrahedral singular (quarter point node) element

The specimen is subjected to an axial tensile load of 100N/mm^2. The material properties of the specimen are

E=2.06E5 N/mm^2 and ν=0.3

The stress-concentration factor is calculated for different pitting intensities as shown in Fig. 4. The stress concentration factor, K_t is in the range of $2<K_t<3$ and agrees well with those of Peterson [10] for 3-dimensional surface defects.

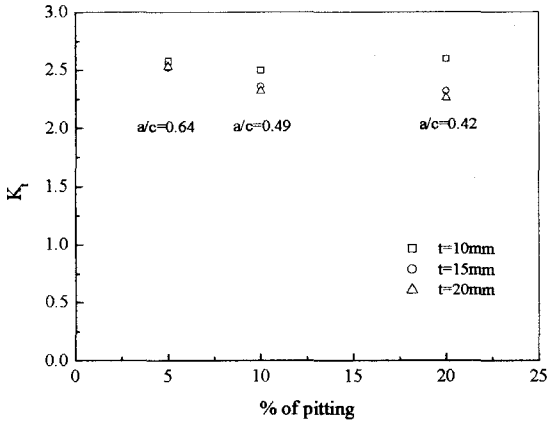

Fig. 4 Variation of stress concentration factor K_t with pitting intensity

2.2 Theory and Numerical Analysis

On computing the stresses in the specimen, the stress intensity factor is computed using the following relation by measuring the stress at the node which is adjacent to the critical node where crack is likely to initiate (point A and

varying intensity of pitting, in specimens with high thickness.

In general, the stress intensity factors are found to decrease with increase in the thickness of the specimen. This decrement is found to be significant in specimens with high intensity of pitting whereas in specimens with lower intensity of pitting have moderate decrease of stress intensity factor with increasing thickness.

3.2 Estimation of stress intensity factor for 3-D surface defects using the formula

Based on the finite element results, the empirical formula is derived to estimate the stress intensity factor for any pit of given size such as pit depth to specimen thickness ratio (a/t) and pit depth to pit diameter ratio (a/c). The formulae are based on regression analysis.

Table 2 Stress Intensity factors at the depth and surface of the pit w.r.t pitting intensity and specimen thickness

Specimen thickness (㎜)	Method	5% pitting a=4.55㎜ 2c=14.14㎜		10% pitting a=5.09㎜ 2c=20.75㎜		20% pitting a=5.72㎜ 2c=27.42㎜	
		K_A	K_B	K_A	K_B	K_A	K_B
10	FEM	455.84	385.17	489.40	396.96	568.43	431.08
	Eq.(2)/ Eq(3)	457.65	386.66	505.45	401.48	560.19	426.95
	Ref.[8]	340.56	320.32	425.21	354.62	511.08	400.94
15	FEM	474.42	392.80	484.71	394.07	536.63	404.99
	Eq.(2)/ Eq(3)	460.32	387.51	484.51	390.43	519.80	406.08
	Ref.[8]	325.05	295.24	392.72	313.67	456.25	339.17
20	FEM	452.86	382.29	465.47	389.05	497.64	393.30
	Eq.(2)/ Eq(3)	461.66	387.94	474.04	384.91	499.61	395.64
	Ref.[8]	319.01	286.15	379.82	298.67	433.96	316.36

Table 2 shows stress intensity factor at the depth and surface of the pit with regard to pitting intensity and thickness of the specimen. The stress intensity factors obtained from the finite element analysis and also using eq.(2) and eq.(3) are compared with those obtained using Newman Raju's method[8].

Figs. 6-8 show the comparison of normalized stress intensity factor obtained using eq.(2) and eq.(3). The formula compares well with finite element solutions for both at point A and point B of the pit.

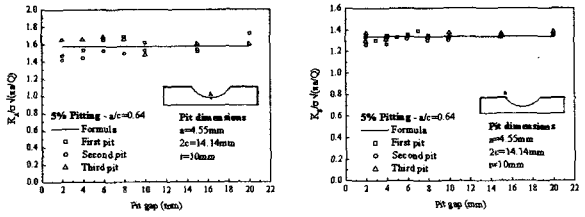

(a) At Point A (b) At Point B

Fig. 6 Stress intensity factors in a specimen subjected to 5%pitting (Thickness, t = 10㎜)

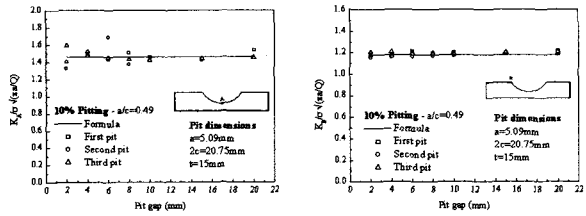

(a) At Point A (b) At Point B

Fig. 7 Stress intensity factors in a specimen subjected to 10%pitting (Thickness, t = 15㎜)

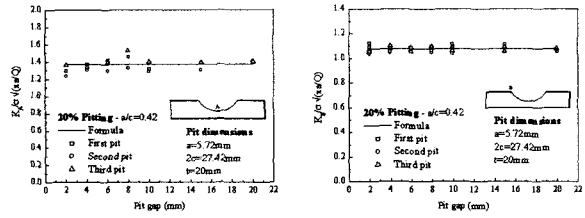

(a) At Point A (b) At Point B

Fig. 8 Stress intensity factors in a specimen subjected to 20%pitting (Thickness, t = 20㎜)

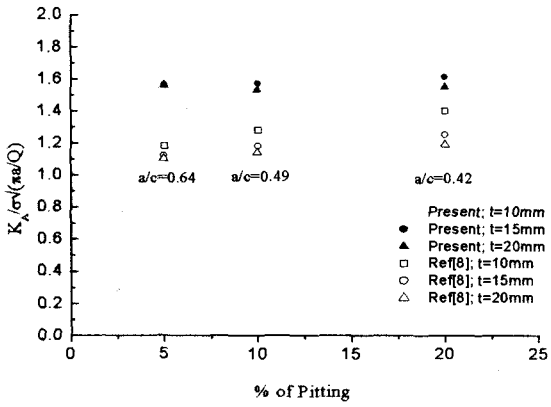

Fig. 9 Stress intensity factor at the depth of the pit (point A) based on empirical formula for 3-dimensional and 2-dimensional surface defects

point B as shown in Fig.1)

$$K = \sigma\sqrt{2\pi r} \quad (1)$$

where K is the stress intensity factor, σ is the nodal stress and r is the radial distance from the crack tip to the node at which stress σ is measured.

2.3 Simplified formula

An empirical formula to estimate the stress intensity factor for 3-dimensional surface defects under axial tensile load is fitted to the finite element results.

Stress intensity factor at the depth of the pit

$$K_A = \sigma\sqrt{\frac{\pi a}{Q}}\left[-2.8308\left(\frac{a}{c}\right)\left(\frac{a}{t}\right)+1.7608\left(\frac{a}{t}\right)+1.8021\left(\frac{a}{c}\right)+0.4497\right] \quad (2)$$

Stress intensity factor at the surface of the pit

$$K_B = \sigma\sqrt{\frac{\pi a}{Q}}\left[-1.4098\left(\frac{a}{c}\right)\left(\frac{a}{t}\right)+0.8878\left(\frac{a}{t}\right)+1.5379\left(\frac{a}{c}\right)+0.3555\right] \quad (3)$$

where

$$Q = 1.0 + 1.464\left(\frac{a}{c}\right)^{1.65}$$

3. Results and Discussion

3.1 FE analysis and result

The stress intensity factors are computed at both the point A and point B of the pit (Fig. 1). Figs. 5a and 5b show the plots of variation of stress intensity of factor with varying a/c ratio. A normalized value of stress intensity factor using the pit depth, a and pit geometry factor, Q is presented in the results. The results are based on the finite element analysis carried in the present investigation. The stress intensity factor is found to increase with pit size. In other words, stress intensity factor is a function of pitting intensity and increases with increase of pitting intensity. The effects of multiple pits is found to be negligible. This may be due the fact that the load is tensile and hence the effects of neighbouring pits are minimal. But this assumption may not hold good under bending loads. The effect of specimen thickness is found to influence the stress intensity factor. It is observed that with increase in thickness of the specimen, the stress intensity factor has reduced.

Figs. 6-8 show the variation of stress intensity factor with respect to pitting intensity, pit depth to pit diameter ratio and specimen thickness.

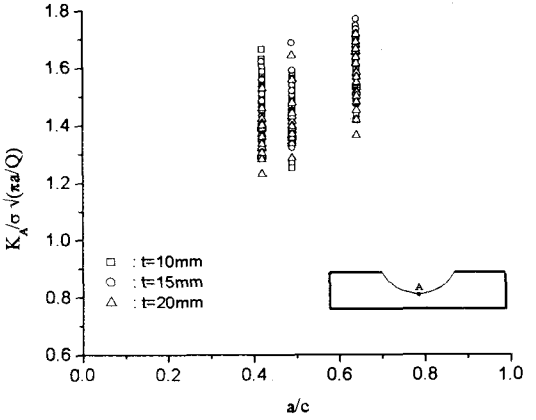

Fig. 5a Variation of stress intensity factor at point A with a/c ratio

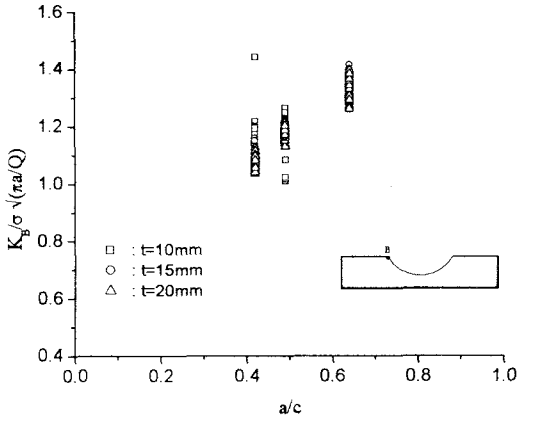

Fig. 5b Variation of stress intensity factor at point B with a/c ratio

Figs. 6a and 6b show the variation of stress intensity factors K_A and K_B w.r.t. pitch, d of pits in a specimen subjected to 5% pitting. Fig. 7 shows the variation of stress intensity factors K_A and K_B in a specimen (t=15㎜) with 10% pitting. Fig. 8 shows a similar plots for specimens subjected to 20% pitting.

The stress intensity factors are found to increase with increase in the percentage of pitting. The stress intensity factors are found to increase moderately with intensity of pitting varying from 5% to 10% whereas the increase is very high from 10% to 20% intensity of pitting. This is significantly noticed in specimens with lower thickness. The percentage of pitting and also the thickness of the specimen influence the stress intensity factor at the depth of the pit (point A) significantly. However, the stress intensity factor at the surface of the pit (point B) is found to be almost invariable, for

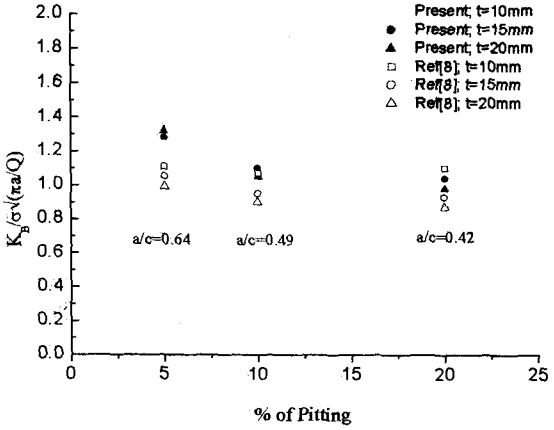

Fig. 10 Stress intensity factor at the surface of the pit (point B) based on empirical formula for 3-dimensional and 2-dimensional surface defects

Figs. 9 and 10 show the comparison of the stress intensity factor which is estimated using the developed formulae and those of Newman and Raju[8]. A significant discrepancy is observed between the two results. This may be due to influence of the 3-dimensional effects of the pit and the stress intensity factor is underestimated using the formulation for 2-D surface defects. However, the behaviour of the two results with respect to pitting intensity is found to be similar.

Figs. 11 and 12 shows the variation of stress intensity factor with varying a/t ratio. The stress intensity factor is found to increase with increasing a/c ratio. The variation is found to be significant at point A with varying a/t ratio (Fig. 11) whereas at point B it is found to be almost invariant (Fig. 12).

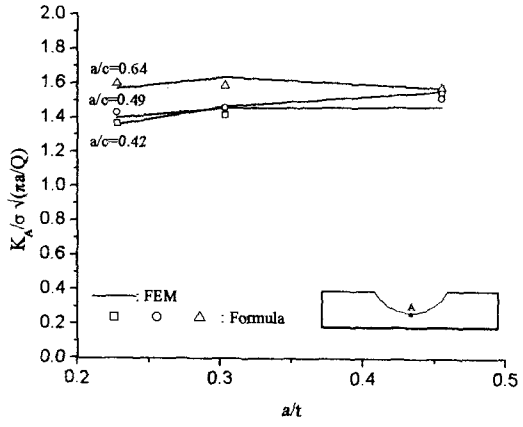

Fig. 11 Variation of stress intensity factor at point A with varying a/t ratio

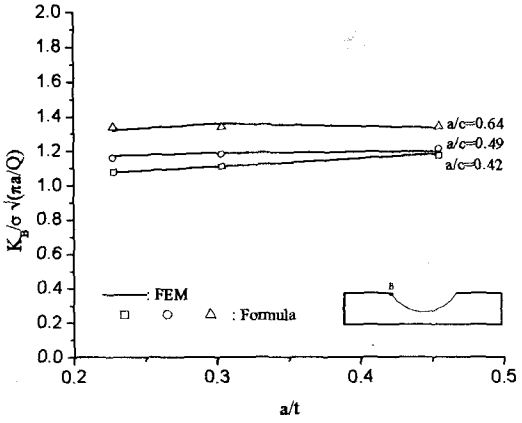

Fig. 12 Variation of stress intensity factor at point B with varying a/t ratio

5. Conclusions

In the present paper, the stress intensity factors are computed for 3-dimensional surface defects such as pits (in marine structures) under axial tensile load. The 10-node tetrahedral elements are used for the finite element model of the specimen and singular elements are used to simulate the crack tip phenomenon. The stress intensity factor is found to decrease with increase in plate thickness and increase with increasing intensity of pitting. The empirical formulae to estimate the stress intensity factor, at the surface of the pit and also at the depth of the pit, are developed by using regression analysis to the results obtained using finite element method. The formula agrees well with 3-D finite element solutions. Moreover, the influence of the 3-dimensional geometry of the surface defect is observed to be significant and the stress intensity factor is underestimated using the formulations of 2-dimensional surface defects. However, the distance between the pits, i.e. pitch of the pit is found to be negligible under axial tensile loads.

References

[1] Chen, G.. S., Wan, K.-C. Wei, R. P. and Flournoy, T. H. (1996). "Transition from pitting to fatigue crack growth modeling of corrosion fatigue crack nucleation in a 2024-T3 aluminum alloy", Materials Science and Engineering, A219, pp. 126-132.

[2] Dolley, E. J., Lee, B. and Wei, R. P. (2000). "The effect of pitting corrosion on fatigue life", Fatigue Fract Engng

Mater Struct, Vol. 23, pp. 555-560.

[3] Hoeppner, D. W. and Chandrasekharan, V. (1998). "Corrosion and corrosion fatigue predictive modeling - State of the art review", Technical Report, FASDE International Inc., USA.

[4] Rokhlin, S. I., Kim, J.-Y., Nagy, H. and Zoofan, B. (1999). "Effect of pitting corrosion on fatigue crack initiation and fatigue life", Engineering Fracture Mechanics, Vol 62, pp.425-444.

[5] Shi. P. and Mahadevan S. (2001). "Damage tolerance approach for probabilistic pitting corrosion fatigue life prediction", Engineering Fracture Mechanics, Vol. 68, pp. 1493-1507.

[6] Simon, L. B. (1999). "Influence of pitting corrosion on the loss of structural integrity in Aluminum alloy 2024-23", M. S. Thesis, University of Dayton, Ohio, USA.

[7] Anderson T.L. (1991). "Fracture Mechanics : Fundamentals and Applications", CRC Press, Boca Raton.

[8] Newman, J. C. and Raju, I. S. (1981). "An empirical stress-intensity factor equation for the surface crack", Engineering Fracture Mechanics, Vol. 15, No. 2, pp. 185-192.

[9] Daidola, J. C., Parente, J. and Orisamolu, I. R. (1997). "Strength Assessment of Pitted Plate Panels", Technical Report: SSC-394, Ship Structure Committee, USA.

[10] Peterson, R. E. (1974). "Stress Concentration Factors", John Wiley & Sons, New York, USA.